Atomic Force Microscopy Studies of Admicellar Polymerization Polystyrene-Modified Amorphous Silica

Chun Hwa See, John O'Haver

Department of Chemical Engineering, The University of Mississippi, University, Mississippi 38677

Received 15 February 2002; accepted 15 April 2002

ABSTRACT: Atomic force microscopy was used to study polystyrene-modified silica surfaces produced by admicellar polymerization (polymerization of monomers solubilized in adsorbed surfactant aggregates). The goal was to examine changes in the location and nature of the formed polystyrene resulting from changes in the surfactant and monomer feed levels on precipitated silica. Normal tapping and phase-contrast modes in air were used to image the topography of the polystyrene-modified silica. Moderate-to-light force-tapping mode was used to differentiate between the silica surface and adsorbed water or polymer. The formed polystyrene exists primarily in the pores, with patches extending onto the exposed surface of the silica particles. At moderate tapping forces, darker phase regions were observed in the valleys and pores of the silica in both the modified and the unmodified samples. Upon higher magnification, the darker regions disappear on unmodified silicas, whereas polymer bands become evident on the modified silicas. At lower loadings of surfactant and monomer, the number and extent of polymer patches decreased, with polymer being found only in pores. The polystyrene patches observed inside the valleys of the amorphous silica varied from 1 to 10 nm in thickness. The structure of the polystyrene film formed on precipitated silica was found to be insensitive to the surfactant feed concentration. © 2002 Wiley Periodicals, Inc. J Appl Polym Sci 87: 290–299, 2003

Key words: atomic force microscopy (AFM); surfactants; thin films; silicas

INTRODUCTION

A thin polymer film formed via admicellar polymerization was used to modify the surface properties of substrates including glass fibers,[1] alumina,[2–4] silica,[5–8] titanium oxide,[9] glass cloth,[10] and nickel flake.[11] O'Haver et al. studied the formation of polymer and copolymer thin films on precipitated silica.[5–8] The modified silica fillers were blended into rubber compounds and tested for various physical, dynamic, and cure properties. The modified silica-filled rubber compounds exhibit decreased cure times and increased break strength, elongation to break, tear strength, and cut-growth resistance.

In these studies, the presence of polymer on the substrate surfaces was indirectly confirmed by various techniques, including scanning electron microscopy (SEM),[2,3] UV analysis of tetrahydrofuran-extracted polystyrene,[4] nitrogen adsorption,[4–8] mercury porosimetry analysis,[3] ellipsometry,[9,10] Fourier transform infrared (FTIR) spectroscopy,[3,8] contact angle analysis, evaluation of properties of the composites produced,[3] and scanning tunneling microscopy.[11] None of these methods provide direct analysis of the structure or extent of the polymer film. A greater understanding of the distribution and characteristics of the polymer film formed by admicellar polymerization could lead to significant improvements in current applications of this technique as well as the development of new applications.

Recent advances in atomic force microscopy (AFM)[12] allow us to study the nanometer scale surface characteristics of substrates. The structure and the location of the styrene-isoprene copolymer film formed via admicellar polymerization has been briefly examined on precipitated silica by O'Haver and coworkers[5] and on polypyrrole film modified nickel flake by O'Rear and coworkers.[11] Both of these studies provided evidence of the existence of polymer on the amorphous substrate, but did little to elucidate how the presence of the polymer film impacts the performance of the modified substrate in rubber compounds. O'Haver et al. found that the performance of modified precipitated silicas as filler in tires depended on the concentrations of the surfactant and monomer. They concluded that the rubber composite performance was optimized when the amount of both the surfactant and the monomer on the surface was low.[13] However, the reason for this was not clear.

Correspondence to: J. O'Haver (johver@olemiss.edu).

Contract grant sponsor: National Science Foundation Award; contract grant number: 9724187; contract grant sponsor: The University of Mississippi Loyalty Foundation; contract grant sponsor: The University of Mississippi Associates and Partners Program.

In this study, we examine the structure and locations of the formed polystyrene film under tapping mode atomic force microscopy (TMAFM) (Digital Instruments Nanoscope IIIa, Santa Barbara, CA) as a function of surfactant and monomer feed concentrations. Amorphous silica (PPG Industries Inc., Pittsburgh, PA) was modified by the admicellar polymerization process by using styrene (Sigma Chemical, St. Louis, MO) adsolubilized in cetyltrimethylammonium bromide (Sigma Chemical, St. Louis, MO) (C_{16}TAB) aggregates. 2,2′-Azobisisobutyronitrile (AIBN) (Aldrich, Milwaukee, WI) was used as the initiator.

Ultrathin film formation

The thin polymer film that is formed via the admicellar polymerization process has been described by several authors.[1–11] The process itself can be described as occurring in the following four distinct steps: (1) surfactant adsorption/admicelle formation, (2) adsolubilization of monomer(s), (3) polymerization, and (4) surfactant removal.

Step 1 is the formation of surfactant aggregates on the substrate surface. These adsorbed surface aggregates, or admicelles, have many micellelike properties and the structure is dependent upon the surface charge as well as the ionic strength of the solution. The structure of the admicelle was observed by using noncontact AFM.[14–26] On a silica surface, spherical or hemispherical C_{16}TAB admicelles have been observed by Liu and Ducker at bulk concentrations two times the critical micelle concentration (CMC) by using repulsive noncontact AFM.[20] With additional electrolyte, they found it possible to change the morphology of the adsorbed aggregates from spheres to cylinders.[21,22] At 90% of the CMC, C_{16}TAB admicelles will form spherical or short cylindrical structures on silica.[22] However, the surfactant concentrations of interest in the admicellar polymerization process are always below the CMC, and no images have been captured of adsorbed cationic surfactant aggregates on amorphous silica in this lower concentration range.

In the second step, adsolubilization, the equilibrium bulk concentration of the surfactant is below the critical micelle concentration. Thus, the relatively hydrophobic monomers preferentially partition into the hydrophobic interior of the admicelle. The monomer can be introduced into the solution at the same time as the surfactant and the initiator or following adsorption.

In step three, polymerization of the monomer(s) is accomplished. During polymerization, the admicelle serves as the primary loci for the *in situ* polymerization, with very little of the reaction occurring in the bulk solution. Wu[2] and Hirt[1] observed that monomer (styrene) continuously diffused into the admicelle during the reaction process, with an exponential decay of the concentration profile versus time shown by both studies. Wu noted that the transport and reaction models were consistent with a system that was initiated and terminated inside the admicelle and that the reaction time decreased with increasing initiator concentration.

In the final step, surfactant is removed by washing with water, exposing the polymer film on the substrate. The modified silica is then dried and processed for use.

EXPERIMENTAL

Materials

A cationic surfactant, cetyltrimethylammonium bromide (C_{16}TAB), 99% pure, was obtained from Sigma Chemical Co. (St. Louis, MO). Hi-Sil 233, an amorphous, precipitated silica with a N_2-BET surface area of 150 m^2 per gram, was obtained from PPG Industries (Pittsburgh, PA). Styrene, 99% purity, was purchased from Sigma. AIBN (99% purity) was obtained from Aldrich (Milwaukee, WI). All materials were used as received. Deionized water with a resistivity of 18.3 MΩ cm was obtained by using a Barnstead E-pure water system.

Atomic force microscopy

The atomic force microscope, a multimode Nanoscope IIIa AFM, was purchased from Digital Instruments, Inc. (Santa Barbara, CA). Topographic and phase images were captured simultaneously by using tapping mode AFM. All imaging was done by using 125-μm silicon tips obtained from Digital Instruments, Inc. A set-point ratio (ratio of the engaged oscillation amplitude to the free air oscillation amplitude) between 0.5 and 0.7 was used for all topographic and phase images unless otherwise stated. With this set-point ratio, darker regions will represent the softer polystyrene film, whereas brighter regions will represent the harder silica substrate.

The thickness of the polystyrene films was analyzed by using the Nanoscope IIIa software version 4.23r23 (Digital Instruments).

The microscope was enclosed within a Plexiglas® box (14 × 14 × 30 in.). Dry air (7 ± 2% relative humidity) was pumped into the container. The relative humidity inside the container was monitored by a humidity probe obtained from Cole-Parmer Instrument Co. (Vernon Hills, IL). All tapping mode images were captured at room temperature and in air with a relative humidity $< 25\%$.

Sample preparation

The silica has a point of zero charge (p.z.c.) between pH 2.0 and 3.0.[27] Because a negatively charged surface

TABLE I
Feed Solutions

Silica samples	$C_{16}TAB$ (μM)	AIBN (μM)	Styrene (μM)	Ratio of the styrene feed concentration of the sample to that of sample AI-1
Experiment set one				
AI-1	12,000	2000	7500	1 : 1
AI-2	6000	2000	3750	1 : 2
AI-3	3000	2000	1875	1 : 4
AI-4	250	2000	375	1 : 20
Silica Samples	$C_{16}TAB$ (μM)	AIBN (μM)	Styrene (μM)	Ratio of adsorbed $C_{16}TAB$ to adsolubilized styrene monomer
Experiment set two				
AII-1	12,000	2000	173.3	2 : 1
AII-2	12,000	2000	86.7	4 : 1
AII-3	12,000	2000	43.3	8 : 1
AII-4	12,000	2000	8.7	40 : 1

would facilitate adsorption of the cationic surfactant, and as silica has a minimum solubility in water at pH 8, a feed solution pH of 8 was chosen. The critical micelle concentration of $C_{16}TAB$, obtained from adsorption isotherm data on amorphous Hi Sil 233,[28] was in the range of 0.8 to 0.9 mM, which compared well with the published value of 0.9 mM.[29] Thus, a $C_{16}TAB$ feed concentration was used in all experiments that would equilibrate at $\sim$ 0.72 mM, as determined by adsorption isotherm data.

The pH of the $C_{16}TAB$, AIBN, and styrene aqueous solution was adjusted to 8 by using a small amount of sodium hydroxide solution and then by mixing with 1 g Hi-Sil 233 in a 20-mL vial and equilibrated for 4 days at 25°C. The vials were then placed into a 70°C water bath for 24 h to accomplish polymerization. After polymerization, the silica was washed with deionized water until no foam could be generated in the wash water. The silica powder was then filtered and allowed to dry overnight in a 40°C oven. The samples of modified amorphous silica were then stored in clean vials inside a desiccator.

The silica powders were mounted for imaging by melting a small amount of the thermoplastic adhesive TEMPFIX (Electron Microscopy Sciences, Washington, PA) at 120°C on a 12-mm metal plate and then by sprinkling the silica on top of the melt layer. After the adhesive solidified at 80°C, excess silica was removed by a flow of dry air.

Two different sets of experiments were prepared: In the first set, varying amounts of a solution with a constant ratio of $C_{16}TAB$ to styrene was used to modify the amorphous silica. In the second set of experiments, the concentration of $C_{16}TAB$ was kept constant at a point just below its maximum adsorption, whereas the concentration of styrene was varied. Four samples were prepared in each experimental set (see Table I).

RESULTS AND DISCUSSION

Unmodified silica

A topographic image of unmodified silica is shown in Figure 1. The observed primary particle sizes range from 20 to 150 nm in diameter with an average diameter of $\sim$ 60 nm. The unmodified silica surface consistently caused $<20°$ in phase shift.

In phase mode, the valleys and edges of the primary particles appear darker, demonstrating that darker regions do not necessarily indicate softer regions on high surface area substrates when operating at a setpoint ratio of 0.5–0.7. This result is in contrast to that of Brandsch et al.[30–32] The tapping frequency can be easily influenced by high surface curvature, thus giving a false reading. At constant tapping oscillation amplitude (constant tapping force), the tip will have to travel longer distances to reach the valleys between the primary particles. To maintain the constant force or constant separation distance between the tip and the surface, the tapping frequency will be delayed. The result of this delay is observed as the lower phase shift on the phase images. As a result, the phase contrast in the valleys between the primary particles will appear to be darker, even without the presence of soft materials such as polymer film. Thus, when darker areas were observed, imaging under different forces was used to determine if the region was polymer or not.

Constant ratio of initial $C_{16}TAB$ and styrene concentrations (sample series of AI)

The first set of samples investigates the structure and location of the formed polystyrene by using a constant

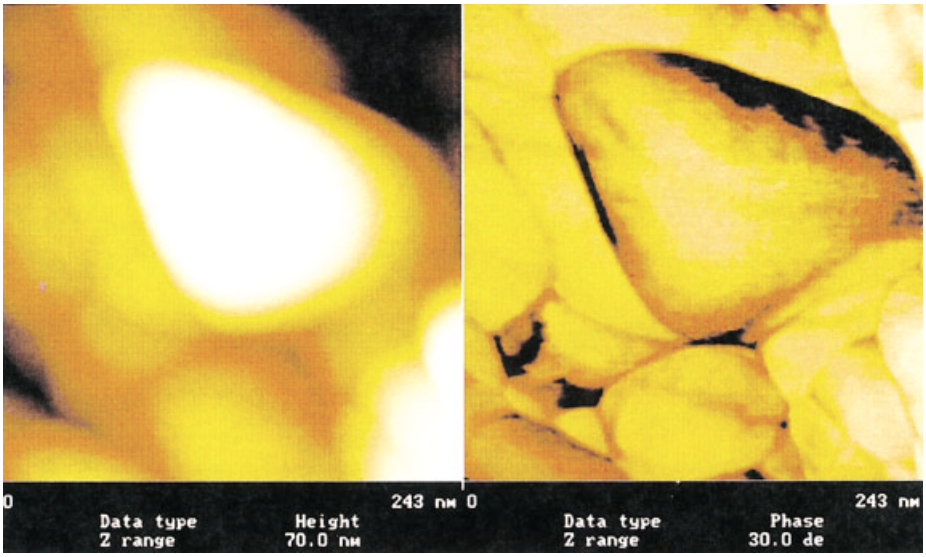

Figure 1 Topographic (left) and phase (right) images of unmodified amorphous silica. Note that on the phase image, darker areas are observed at the valleys and the surface with a negative curvature. Scan size of 243 × 243 nm^2 with *z*-scale of 70 nm and 30° in phase images.

C_{16}TAB-to-styrene ratio in the feed for the admicellar polymerization process. The topographic and phase images of sample AI-I (Fig. 2) clearly show the presence of polystyrene aggregates, although there is little significant difference in phase contrast. The size of the observed primary silica particles is much larger than those of the unmodified silica, hundreds of nanometers, compared to an average size of 60 nm in unmodified silica. Thus, it appears that the primary particles are encapsulated by a relatively thick layer of polystyrene film, forming a homogenous surface that does not show much phase contrast. In addition to the film, polystyrene aggregates were observed adsorbed on top of the encapsulated silica. These aggregates were formed either by spontaneous agglomeration of the polystyrene film before drying or by the dewetting mechanism of the polystyrene film during and after drying. These polystyrene aggregates vary from 30 to 70 nm in size and are scattered around the coated-silica surface as well as within the valleys between the primary silica particles.

The formation of these aggregates was observed only at high feed concentrations of styrene. From a study by O'Haver et al.,[8] the feed conditions used for

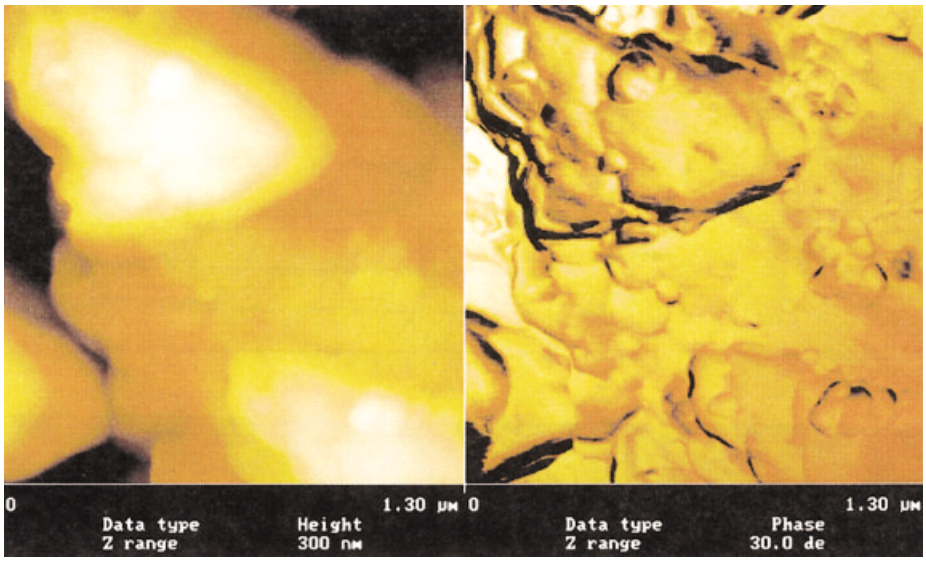

Figure 2 Topographic (left) and phase (right) images of modified amorphous silica with the initial concentration of C_{16}TAB of 12 mM and styrene of 7.5 mM (sample AI-1). Imaging size of 1.30 × 1.30 μm^2 with *z*-scale of 300 nm and 30° in phase images.

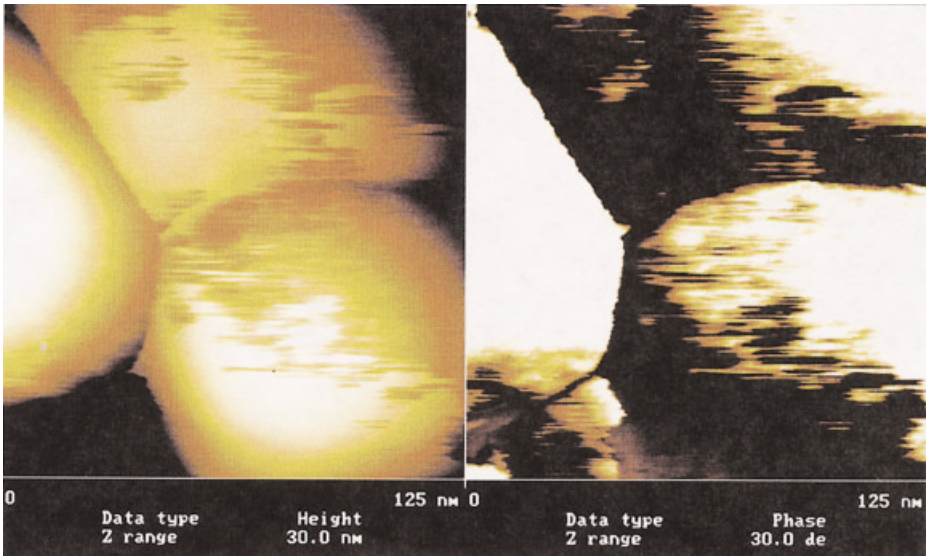

Figure 3 Topographic (left) and phase (right) images of modified amorphous silica with the initial concentration of C_{16}TAB of 6 mM and styrene of 3.75 mM (sample AI-2). Imaging size of 125 × 125 nm^2 with *z*-scale of 30 nm and 30° in phase images.

these samples should create a styrene-saturated admicelle. As additional monomer diffuses in during polymerization and the polymer aggregate grows, phase separation of the polymer becomes possible (Wu[2,3] and Hirt[1]). The same phenomenon has been extensively investigated by El-Aasser et al. in miniemulsions, where predissolved polystyrene was used to increase the rate and total amount of styrene solubilized.[33–35] Adsorbed C_{16}TAB reduces the interfacial energy, and thus, when the C_{16}TAB is washed away, the polystyrene will agglomerate to minimize the interfacial energy. This could result in the spherical or oval aggregates observed in the topographic image.

In sample AI-2, a thin, noncontinuous polystyrene film was observed. This film is concentrated primarily in the pores and valleys of the silica, but also extends in places onto the surface (Fig. 3). The polystyrene film can be clearly distinguished as the darker areas in the phase image. The thickness of the polystyrene film varies from 4 to 7 nm as determined by the Nanoscope III software. The AFM is able to discern films as thick as a few angstroms, both by topography and by the ability of the tip to deform the film. Thus, we are confident that the film is noncontinuous and located only where observed. The variation in thickness and location may be caused by a larger amount of monomer being present in the pores, as the pore space makes up the majority of the surface area of the solid, or due to drying effects where the thin film is dragged off of the surface and into the pores by the retreating liquid films.

As the initial concentrations of both C_{16}TAB and styrene were further decreased, the area covered by the polystyrene film decreased, making it more difficult to locate the polystyrene film with TMAFM. Because the majority of the formed polymer will be located inside pores into which the AFM may not be able to penetrate, polymer present on the surface of the silica may be difficult to find. Additionally, if the film is too thin, the tip may actually deform and/or remove the film from the silica surface. To avoid the problems associated with phase imaging and to increase the detection limits, lighter tapping forces were applied on samples with low C_{16}TAB and styrene monomer loadings.

In sample AI-4, a uniform polystyrene film was observed in the valleys between the primary particles of silica (Fig. 4). The phase image shows the location of the polystyrene film as darker regions compared to the silica substrate. Besides analyzing the topographic and phase images, the presence of the polystyrene film was also confirmed by the technique of imaging under different forces. In this technique, the same area was imaged by using significantly different imaging forces. In using moderate tapping force, we are able to observe the darker patches that indicate the polystyrene strands. When the applied force is increased, the tip is able to deform or remove these strands if the polymer is thin or soft. When a portion of the polymer strands has been removed or deformed, the darker strands observed in the phase image and the higher strands observed previously in topography mode will disappear, confirming the presence of soft and deformable polystyrene strands.

The polystyrene thin film can be easily deformed or removed by increasing the tapping force from a setpoint ratio of 0.9 to 0.5. Figure 5 shows the same location as Figure 4 after imaging with a higher tapping force. The polymer film has been removed, exposing the homogeneous silica surface. It must be

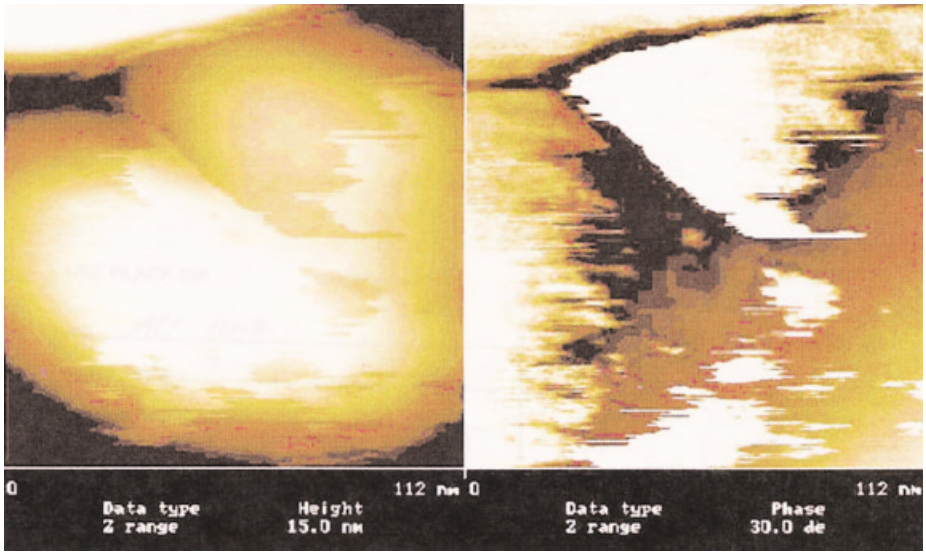

Figure 4 Topographic (left) and phase (right) images of modified amorphous silica with the initial concentration of C_{16}TAB of 2.5 mM and styrene of 0.375 mM (sample AI-4). Imaging at set-point ratio of 0.9. Imaging size of 112 × 112 nm^2 with *z*-scale of 15 nm and 30° in phase contrast.

noted, however, that the darker region in Figure 4 between two primary particles represents a valley of <30° in the phase shift. Thus, the darker region observed in the phase image is due to its surface curvature or adsorbed water and not to any soft polymer film.

Varying initial concentration of styrene (sample series AII) with constant surfactant loading

In the second sample series, the initial concentration of C_{16}TAB was kept constant at 12 mM, whereas the styrene loading varied from 173.3 to 8.7 μM. Thus, surfactant coverage was maintained at maximum adsorption while reducing the amount of adsolubilized monomer.

When the styrene feed concentration was high (C_{16}TAB concentration 12 mM, styrene concentration 173.3 μM, sample AII-1), the polystyrene thin film appears as the darker region in the phase image at moderate tapping force (Fig. 6). The 3-D topography image of sample AII-1 shows that the polystyrene film

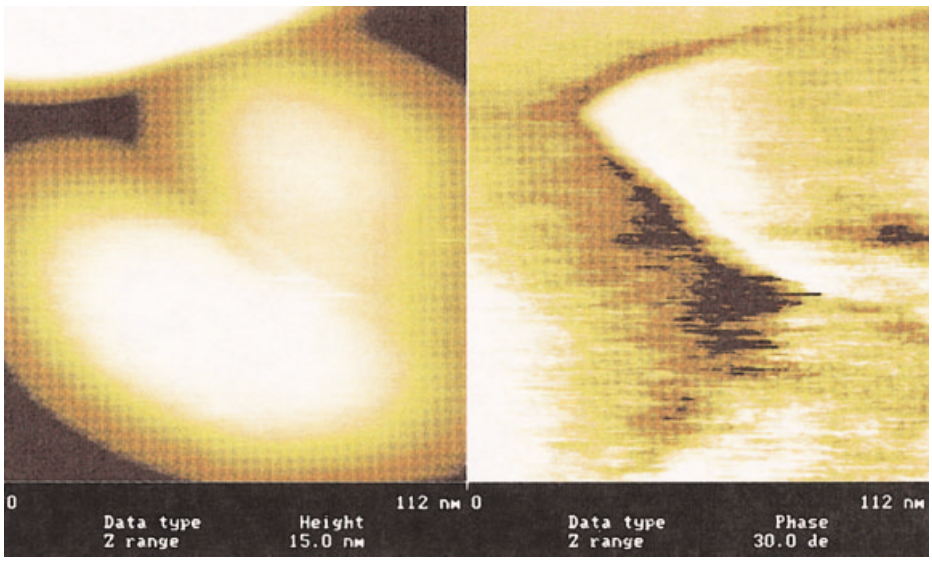

Figure 5 Topographic (left) and phase (right) images of modified amorphous silica with the initial concentration of C_{16}TAB of 2.5 mM and styrene of 0.375 mM (sample AI-4). Imaging at set point of 0.5 at same location as in Figure 4; most of the polystyrene film is removed after scanning at higher force. Imaging size of 112 × 112 nm^2 with *z*-scale of 15 nm and 30° in phase contrast.

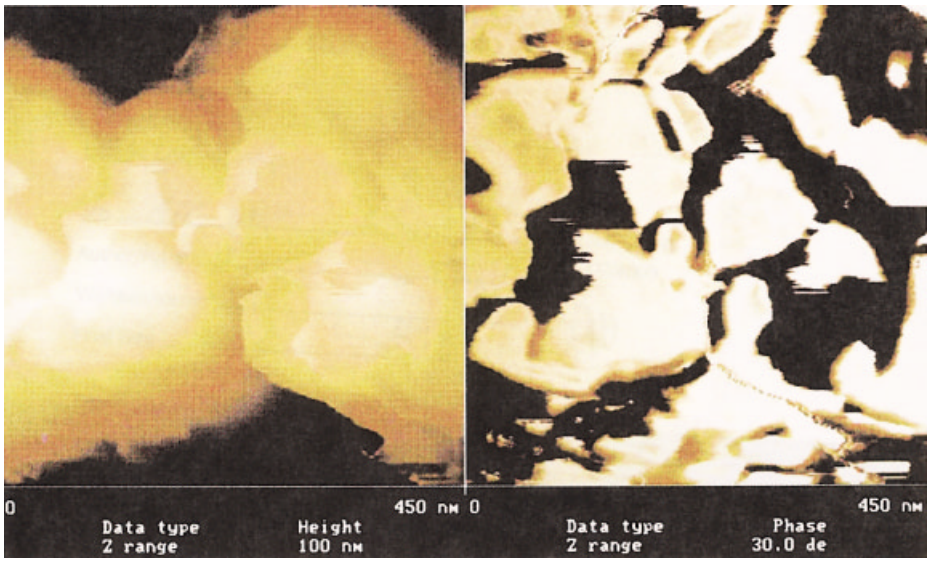

Figure 6 Topographic (left) and phase (right) images of modified amorphous silica with the initial concentration of C_{16}TAB of 12 mM and styrene of 173.3 μM (sample AII-1). The scanning size is 450 $\times$ 450 nm^2 with z-scale of 100 nm and 30°. The dark contrast showing in the phase image indicates the location of the polystyrene strand.

extends from the depressions between primary particles out onto the exposed surface (Fig. 7). The thickness of the polystyrene films is $\sim$ 6 nm.

The structure of the polystyrene film on sample AII-2 (initial styrene feed 50% of that of sample AII-1) is virtually identical to that of sample AII-1. Figure 8

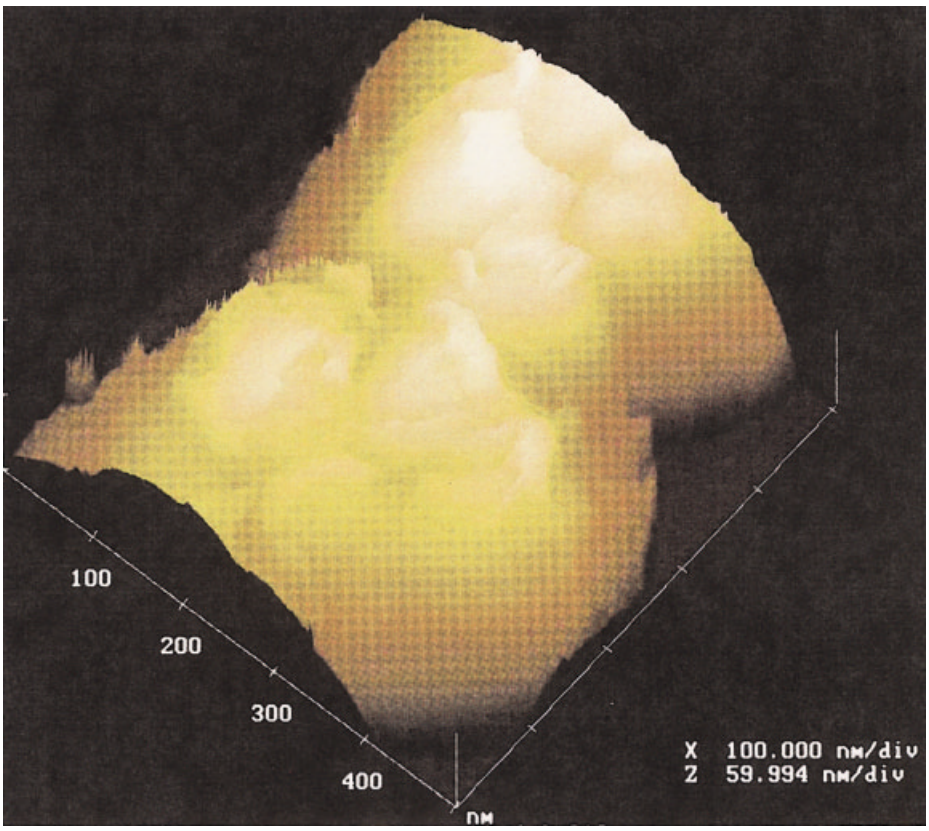

Figure 7 3-D images of modified amorphous silica with the initial concentration of C_{16}TAB of 12 mM and styrene of 173.3 μM (sample AII-1). Imaging size is 450 $\times$ 450 nm^2 with z-scale of 50 nm. This image shows the extended polystyrene strand from inside the valley.

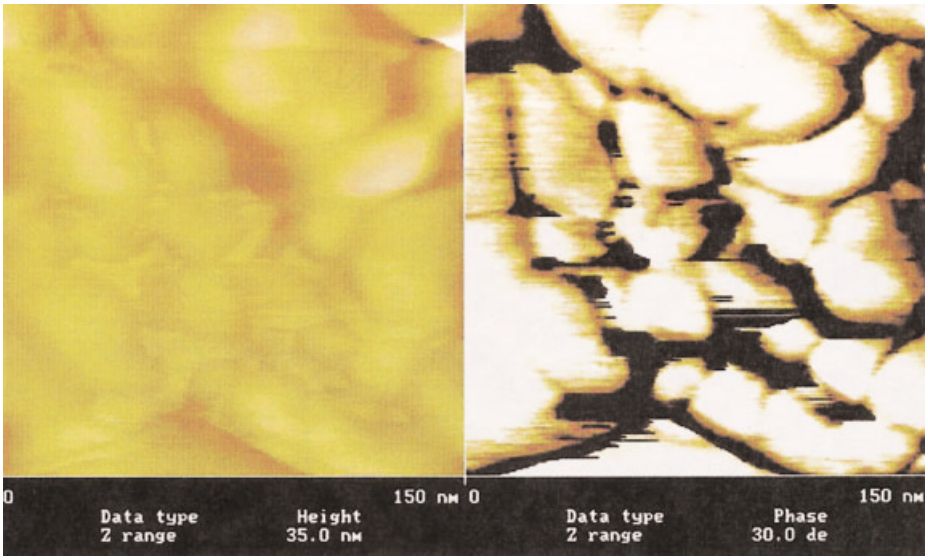

Figure 8 Topographic (left) and phase (right) images of modified amorphous silica with the initial C_{16}TAB concentration of 12 mM and styrene concentration of 86.7 μM (sample AII-2). Imaging size is 150 $\times$ 150 nm^2 with z-scale of 35 nm and 30°. The dark contrast showing in the phase image indicates the location of the polystyrene strand.

shows the topography and phase image of sample AII-2. However, by measuring the local thickness at various points and by comparing with sample AI-1, the extent of the polystyrene film observed in sample AII-2 is much less.

In sample AII-3 (initial styrene feed concentration 26% that of sample AII-1), thin polystyrene strands can be observed near the valleys in the phase image, but are hardly distinguishable in the topographic image (Fig. 9). A large area of the surface, as seen in the phase image, appears to have phase shift of at least 30° near the valleys at moderate tapping force. We can conclude that those areas are covered by a thin layer of polystyrene film, so thin that we are unable to differentiate its existence from the topographic image associated with sharp curvature of the silica. The average thickness of the strands therefore cannot be determined.

As the styrene feed concentration is further reduced to 8.7 μM, it becomes increasingly difficult to locate polystyrene strands on the silica surface, even in the valleys. In sample AII-4 (Fig. 10), where the styrene feed is 5% of that of sample AII-1, we observe polystyrene film not uniformly scattered on

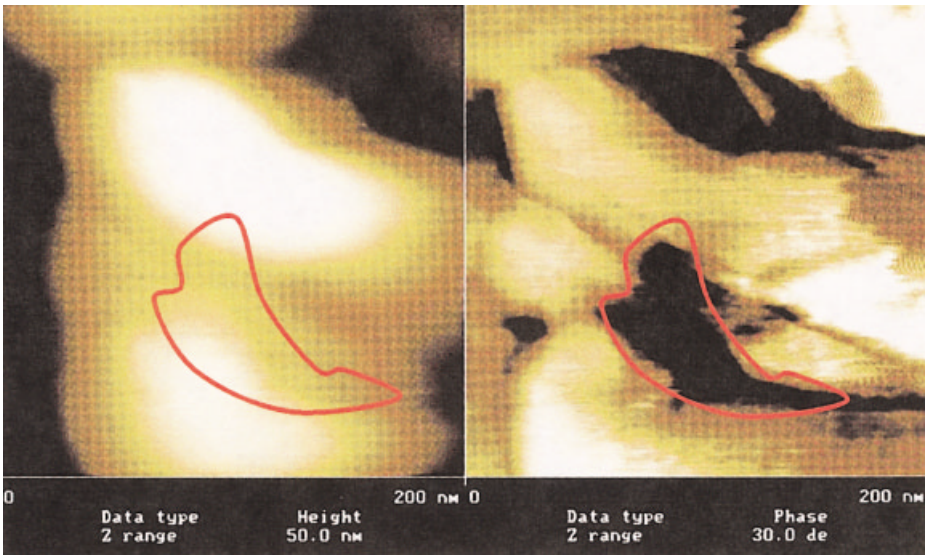

Figure 9 Topographic (left) and phase (right) images of modified amorphous silica with the initial C_{16}TAB concentration of 12 mM and styrene concentration of 43.3 μM. The scanning size of the topographic image is 200 $\times$ 200 nm^2 with height scale of 50 nm and 30° in phase shift. The polystyrene band can be easily seen in the phase image enclosed by the red circle but is hardly observed in the topographic image.

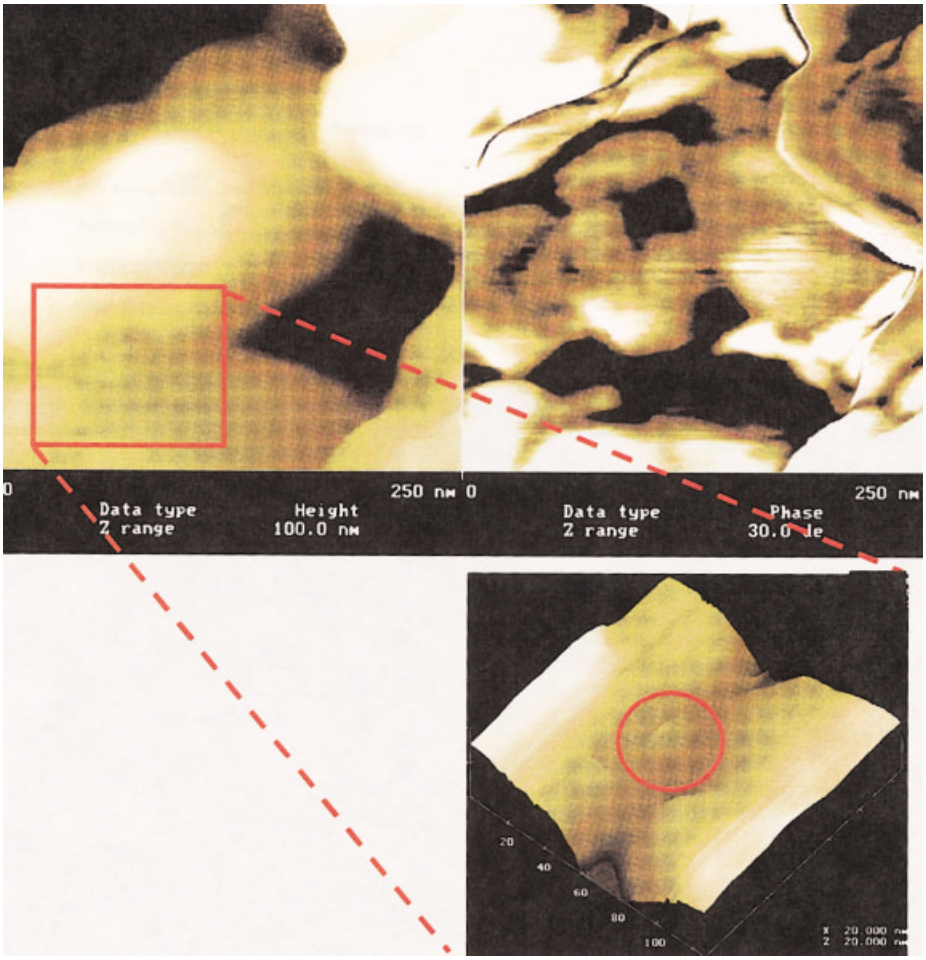

Figure 10 Topographic (left) and phase (right) images of modified amorphous silica with the initial concentration of C_{16}TAB of 12 mM and styrene of 8.7 μM. Imaging size is 250 $\times$ 250 nm^2 with z-scale of 100 nm and 30°. Enclosed is the enlarged 3-D image with imaging size of 125 $\times$ 125 nm^2, z-scale of 20 nm. The polystyrene aggregate anchor at the pores between two primary silica particles with thickness $\sim$ 3 nm was shown with the enclosed red circle.

the silica surface but only concentrated inside the pores. The observed thicknesses vary from $<$1 nm up to $>$3 nm.

The formation of these polystyrene aggregates at the pores may have two causes. One is that the polystyrene film may be forming on the exposed silica surface, but during the washing and drying process, the interfacial tension of the receding liquid pulls the polystyrene film into the pores. If the film is anchored by extending deep into the pore, the surface film should agglomerate at the mouth of the pore and will not be removed during the washing phase. If the film is not anchored, it may be removed during washing, even though it agglomerates during drying. A second reason for so little polymer on the exposed surfaces related to surface area is that the vast majority of the surface area is internal and thus little film is formed on the exposed surface.

The thickness of the polystyrene film was found to be directly proportional to the styrene feed concentration up to a ratio of adsorbed C_{16}TAB to adsolubilized styrene of 40 : 1. At this ratio, the film is no longer stable and aggregates form.

CONCLUSION

Tapping-mode atomic force microscopy reveals the morphology of the polymer film formed via admicellar polymerization on amorphous silica. At a tapping set-point ratio between 0.5 and 0.9, we are able to locate the presence of the polymer strands on the amorphous silica through topographic and phase images. At high styrene loadings, the polymer tends to form aggregates, whereas at lower loadings of both surfactant and styrene, a thin film forms. The morphology of the polymer film does not change significantly when the surfactant feed is kept constant. The thickness of the polymer film is directly proportional to the styrene feed level. At extremely low styrene feed concentrations, polymer tends to aggregate near

the mouths of the pores of the silica aggregates. The presence of polymer aggregates primarily at the entrance to pores may be due to the dewetting process and to the large surface area present in the pores. The formation of surface aggregates at high concentration that may be removed by shear gives some insight into why high loadings of surfactant and monomer produced silicas that did poorly in rubber reinforcement, whereas low loadings, which primarily formed polymer in the silica pores that would not be easily removed, showed the best performance. Future work is needed to examine the impact of the structural aggregates on the performance of the modified silicas in rubber compounds.

The authors thank The National Science Foundation (Award No. 9724187), The University of Mississippi Loyalty Foundation, and The University of Mississippi Associates and Partners Program for providing funding of this project.

References

1. Sakhalkar, S. S.; Hirt, D. E. Langmuir 1995, 11, 3369.
2. Wu, J. Y.; Harwell, J. H.; O'Rear, E. A. J Phys Chem 1987, 91, 623.
3. Wu, J. Y.; Harwell, J. H.; O'Rear, E. A. AIChE J 1988, 34 (9), 1511.
4. Lai, C. L.; Harwell, J. H.; O'Rear, E. A. Langmuir 1995, 11, 905.
5. Waddell, W. H.; O'Haver, J. H.; Evans, L. R.; Harwell, J. H. J Appl Polym Sci 1995, 55, 1627.
6. Thammathdanukul, V.; O' Haver, J. H.; Harwell, J. H.; Osuwan, S.; Na-Ranong, N.; Waddell, W. H. J Appl Polym Sci 1996, 59, 1741.
7. O'Haver, J. H.; Harwell, J. H.; Evans, L. R.; Waddell, W. H. J Appl Polym Sci 1996, 59, 1427.
8. O'Haver, J. H.; Harwell, J. H.; O'Rear, E. A.; Snodgrass, L. J.; Waddell, W. H. Langmuir 1994, 10, 2588.
9. Chen, H. Y. Master's Thesis, University of Oklahoma, 1992.
10. Grady, B. P.; O'Rear, E. A.; Penn, L. S.; Pedicini, A. Polym Composites 1998, 19, 579.
11. Genetti, W. B.; Yuan, W. L.; Grady, B. P.; O'Rear, E. A.; Lai, C. L.; Glatzhofer, D. T. J Mater Sci 1998, 33, 3085.
12. Binnig, G.; Quate, C. F.; Gerber, Ch. Phys Rev Lett 1986, 56 (9), 930.
13. O'Haver, J. H.; Reynolds, J.; Harwell, J. H.; Grady, B. P.; Evans, L. R.; Waddell, W. H. Abstracts, 219th ACS National Meeting, San Francisco, CA, March 26–30, 2000.
14. Fragneto, G.; Thomas, R. K.; Rennie, A. R.; Penfold, J. Langmuir 1996, 12, 6036.
15. Rennie, A. R.; Lee, E. M.; Simister, E. A.; Thomas, R. K. Langmuir 1990, 6, 1031.
16. Manne, A.; Gaub, H. E. Science 1995, 270, 1480.
17. Ducker, W. A.; Wanless, E. J. Langmuir 1996, 12, 5915.
18. Ducker, W. A.; Wanless, E. J. Langmuir 1999, 15, 160.
19. Lamont, R. E.; Ducker, W. A. J Am Chem Soc 1998, 120, 7602.
20. Liu, J.-F.; Ducker, W. A. J Phys Chem B 1999, 103, 8558.
21. Velegol, S. B.; Fleming, B. D.; Biggs, S.; Wanless, E. J.; Tilton, R. D. Langmuir 2000, 16, 2548.
22. Subramaniam, V.; Ducker, W. A. Langmuir 2000, 16, 4447.
23. Sharma, B. G.; Basu, S.; Sharma, M. M. Langmuir 12, 6506.
24. Schulz, J. C.; Warr, G. G. Langmuir 2000, 16, 2995.
25. Sharma, R. in Small-Molecule Surfactant Adsorption, Polymer Surfactant Adsorption, and Surface Solubilization: An Overview; Ravi, S., Ed.; Surfactant Adsorption and Surface Solubilization; American Science Society: 1995; p 1–20.
26. Chen, Y. L.; Chen, S.; Frank, C.; Israelachvilli, J. J Colloid Interface Sci 1992, 153, 244.
27. Iler, R. K. The Chemistry of Silica: Solubility, Polymerization, Colloid and Surface Properties, and Biochemistry; Wiley: New York, 1979.
28. Dickson, J. Master's Thesis, University of Mississippi, 2001.
29. Rosen, M. J. Surfactants and Interfacial Phenomena, 2nd ed.; Wiley: New York, 1989.
30. Bar, G.; Brandsch, R.; Whangbo, W. H. Langmuir 1998, 14, 7343.
31. Brandsch, R.; Bar, G.; Whangbo, W. H. Langmuir 1997, 13, 6349.
32. Whangbo, M. H.; Bar, G.; Brandsch, R. Surf Sci 1998, 411, L794.
33. Blythe, P. J.; Morrison, B. R.; Mathauer, K. A.; Sudol, E. D.; El-Aasser, M. S. Langmuir 2000, 16, 898.
34. Blythe, P. J.; Morrison, B. R.; Mathauer, K. A.; Sudol, E. D.; El-Aasser, M. S. Macromolecules 1999, 32, 6944.
35. Blythe, P. J.; Morrison, B. R.; Mathauer, K. A.; Sudol, E. D.; El-Aasser, M. S. Macromolecules 1999, 32, 6952.